INTERNATIONAL JOURNAL FOR NUMERICAL METHODS IN FLUIDS, VOL. 17, 1003–1013 (1993)

SIMULATION OF VORTEX SHEDDING INCLUDING BLOCKAGE BY THE RANDOM-VORTEX AND OTHER METHODS

P. K. STANSBY AND A. SLAOUTI*

Department of Engineering, Simon Building, University of Manchester, Manchester M13 9PL, U.K.

SUMMARY

Converged simulations of vortex shedding from a circular cylinder at a Reynolds number of 100 have been computed by the random-vortex method incorporating the influence of blockage. The results are compared with converged finite-element and spectral methods and close agreement for Strouhal number is obtained. Forces are, however, in less close agreement, particularly the fluctuating lift force. Strouhal numbers from simulations with zero blockage for Reynolds numbers between 60 and 180 are seen to be in very close agreement with experiments which are said to be effectively two-dimensional. In this range the Strouhal number changes from 0·135 to 0·191. There are no corresponding experimental measurements for force.

KEY WORDS Vortex shedding Laminar flow Numerical simulation Blockage

1. INTRODUCTION

While computational fluid dynamics has developed considerably over the last decade, with three-dimensional computations now quite commonplace, there remains a need for convergence checks for well-defined problems by a range of formulations, particularly for unsteady flows. In two dimensions impulsively started flows around a circular cylinder have received considerable attention by finite-difference methods,[1–3] vortex methods,[4–6] perturbation solutions[7,8] and experiment.[9] There is encouragingly close agreement between results from all methods and experimental measurements of these flows, which are considered to be two-dimensional before the onset of three-dimensional instabilities which occur at a time dependent on the Reynolds number. After some time, vortex shedding occurs; clouds of vorticity of alternating rotation are shed periodically with a frequency, or Strouhal number, which depends on the Reynolds number. This has recently been the subject of much experimental[10,11] and numerical[12–15] work. Experimental evidence indicates that a wake may be produced which remains two-dimensional up to a Reynolds number of 160–180, while numerical studies which allow three-dimensional flow[14] indicate that this is about 200. The difference is probably due to the inevitable background disturbances which must be present in any physical experiment.

In this paper, drag and lift forces and Strouhal number will be compared at a Reynolds number of 100 for finite-element,[12] spectral finite-difference,[13] spectral element[14] and vortex methods where convergence of the numerical method has been claimed. In addition, we consider the question of blockage. Often the cylinder is placed in a rectangular domain with its centre half-way

* Now at Department of Mechanical Engineering Design and Manufacture, Manchester Metropolitan University.

0271–2091/93/231003–11$10.50

Received November 1992
Revised August 1993

between the walls with the zero normal velocity condition. It is tacitly assumed that the distance between the walls has little effect provided it is large, e.g. 16 diameters.[12] This would not be the case for blockage corrections based on steady flow conditions[16] where e.g. a blockage ratio (the ratio of the distance between walls to diameter) of 14 would give an effective increase in free stream velocity of about 4 per cent for a cylinder at a Reynolds number of 10^4.[17] This would cause an increase in drag of about 8 per cent. Clearly this is a substantial quantity which suggests blockage should be taken into account when comparing different numerical schemes, although the postulated blockage correction for steady flow is unlikely to be the same as that in two-dimensional, unsteady flow. In this paper we compute flows using the random-vortex method with blockage ratios of effectively infinity, 16, 8, 4 and 2, although the latter two values in fact bear little relation to the main theme of this paper and are more for general interest.

RANDOM-VORTEX METHOD

This method has been widely applied and will only be summarized here with a description of the method for imposing blockage. Also, two methods for calculating force will be outlined.

Following Chorin,[18] the vorticity equation

$$\frac{\partial \omega}{\partial t} = -(\mathbf{u} \cdot \nabla)\omega + \nu \nabla^2 \omega, \tag{1}$$

where ω is vorticity, t is time, $\mathbf{u}$ is velocity and ν is kinematic viscosity, is split into a linear diffusive part

$$\frac{\partial \omega}{\partial t} = \nu \nabla^2 \omega \tag{2}$$

and a non-linear convective part

$$\frac{\partial \omega}{\partial t} = -(\mathbf{u} \cdot \nabla)\omega, \tag{3}$$

which are solved consecutively at each time step.

At each time step, discrete (point) vortices are introduced around the cylinder surface with strengths which satisfy the zero-slip condition. Diffusion is simulated by imposing random walks to each vortex in two orthogonal directions, the random walks being taken from a normal distribution with zero mean and variance $2\nu\Delta t$, where Δt is time-step size. Vortices which 'walk' inside the cylinder surface are removed rather than reflected in the interests of computational efficiency.[6] This entails an adjustment to the random-walk distribution for the surface vortices. Convection is then imposed by calculating the velocities of each vortex and moving in a first- or second-order Euler scheme.[4-6] Velocities are in this case computed using the vortex-in-cell method,[5,6] which has some advantages for imposing the cylinder surface boundary conditions and effectively gives each vortex a core as its vorticity is spread on to adjacent mesh points so that a Poisson's equation $\nabla^2 \psi = -\omega$ for stream function ψ may be computed. Converged solutions of inviscid vorticity dynamics have been shown to be given by convecting vortices with overlapping cores.[19] Accurate solutions may require many vortices to be generated (e.g. up to 10^5) and the vortex-in-cell method is an efficient method for calculating the velocity of these vortices. The nature of blockage is determined by the mesh configuration.

A single polar mesh in which the radial spacing increases exponentially with distance from the cylinder is used to give the infinite blockage ratio case with the uniform flow condition imposed at the outer boundary, which is a large distance from the cylinder. To give finite blockage an

overlapping system of rectangular and polar meshes will be used;[15] see Figure 1. The outer mesh and the intermediate mesh are rectangular and the inner mesh is polar, as above. Uniform flow conditions are imposed on the upstream and downstream boundaries of the outer mesh and constant stream function values are imposed on the upper and lower boundaries. The meshes are solved sequentially and the velocity of a vortex is calculated from a mesh with the finest mesh size. In this configuration the constant stream function on the cylinder is computed through a boundary-integral calculation from a knowledge of the tangential velocities on the surface. This then gives a coarse distribution of vortices on the surface which enables the stream function at the cylinder centre to be computed accurately, and this value is the value for the cylinder surface and its interior. These coarse vortices are then removed and surface vortices are computed accurately as for a single mesh. The influence matrix for the boundary-integral calculation requires the influence of infinite arrays of periodically spaced vortices (given in Lamb,[20] p. 224) at points around the surface. This is the only modification to the method given in Reference 15.

Finally, two ways of calculating force have been used. First the force is obtained from the pressure distribution around the cylinder; pressure change across a surface segment is conveniently given by the rate of change of circulation on that segment.[5] Skin friction force is obtained from the surface shear stress which is proportional to surface vorticity. With the random-walk method there is an inevitable random component in the force and an alternative scheme has been used in an attempt to reduce this and also to provide an internal check on the numerical scheme.

Napolitano and Quartepelle[21] have given a method for calculating force based on surface and contour integrals involving vorticity in the entire flow field. For the random-vortex method this reduces to a particularly convenient form for the case of a circular cylinder. Defining a Cartesian co-ordinate system with origin at the cylinder centre, x in the onset flow direction and y in the cross-flow direction, the force in the x direction is given by

$$F_x = \sum_{i=1}^{N} \Gamma_i \left[\frac{u_i \sin(2\theta_i) - v_i \cos(2\theta_i)}{r_i^2} \right] + 2F_{xs}, \tag{4}$$

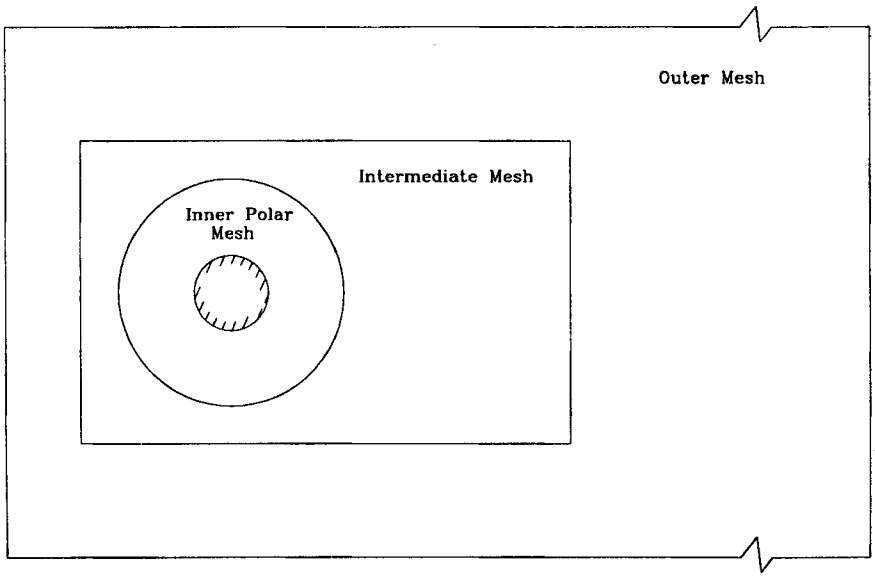

Figure 1. Sketch of overlapping mesh system

where the ith vortex has a position in polar co-ordinates r_i, θ_i, velocity components in the x and y directions of u_i, v_i and vortex strength Γ_i. F_{xs} is the force due to surface shear stress (skin friction) in the x direction.

The force in the y direction is given by

$$F_y = -\sum_{i=1}^{N} \Gamma_i \left[\frac{v_i \sin(2\theta_i) + u_i \cos(2\theta_i)}{r_i^2} \right] + 2F_{ys}, \tag{5}$$

where F_{ys} is the force due to surface shear stress in the y direction.

Without F_{xs} and F_{ys} the force reduces to that given by the well-known Blasius formulation for inviscid flow.

A practical consideration in the numerical calculation concerns the point in the time step at which values of r, θ, u, v should be calculated. The surface vorticity and hence the vortices on the surface are generated during a given time step and hence force computed from the pressure integration and surface vorticity integration relates to the midpoint of that time step. This detail is hardly noticeable in steady onset flow but it can become noticeable in sinusoidal onset flow, where the phase of the force in relation to the onset flow is important.[22] For the above force calculation (hereafter referred to as the QN method) to be compatible, average values of r, θ, u, v for the time step are used.

RESULTS

Results are presented in terms of steady drag (total and skin friction), fluctuating lift and the Strouhal number. The fluid density, cylinder radius and onset velocity are all set to unity and the forces thus relate to the conventionally defined drag and lift coefficients. The Strouhal number S is, however, conventionally normalized by cylinder diameter and is thus twice the lift frequency normalized in this way.

Previous experience with starting flows[5] has indicated that convergence is more dependent on the number of vortices introduced than on the magnitude of the time step. A radial mesh configuration is defined by the number of angular segments, the radial mesh spacing at the surface, the outer domain radius and the number of radial segments. One hundred and twenty-eight angular segments and a radial mesh spacing at the surface equal to the standard derivation of random walk gave converged solutions, including separation prediction, at Reynolds numbers much higher (e.g. 500) than those of interest here (60–180).[5,6] We nevertheless carried out some further convergence studies up to time 20 at $Re = 100$. The second-order vortex convection time-stepping scheme was used throughout. The number of vortices introduced is now determined by a maximum possible vortex circulation magnitude $\Delta\Gamma$. If circulation required at a surface node is Γ, then $(1 + |\Gamma|/\Delta\Gamma)$ vortices are introduced. Values of mean total and skin friction drag, averaged over time 10–20, are given in Table I. These results were in fact obtained with the cylinder between parallel walls 32 radii apart (the spatially periodic situation). A value of $\Delta\Gamma = 0{\cdot}0015$ has been used previously[15] and values of 0·001 and 0·0005 were tested with Δt in the range 0·02–0·1. In general, the results are very close although a slight flow asymmetry has developed. The values of total drag calculated by the QN method are within 0·012 and the skin friction drag values are within 0·010. The conventional total drag calculation (with pressure and surface shear integration) differs from the QN value quite markedly with $\Delta t = 0{\cdot}02$ and $\Delta\Gamma = 0{\cdot}001$. This difference becomes small with $\Delta\Gamma = 0{\cdot}0005$ and is due to insufficient vortices being created on the surface to define surface vorticity adequately. It is thus necessary to reduce $\Delta\Gamma$ as Δt is reduced. The rms fluctuating drag and lift are greater for the conventional calculation than for the QN method because the random noise is less for the latter method. This will be seen below.

Table I. Forces without the imposed asymmetry, averaged over time 10–20 to show dependence on numerical parameters ($Re = 100$)

Numerical parameters		Forces					
Δt	$\Delta\Gamma$	Mean drag	Mean skin friction drag	Rms drag	Mean lift	Rms lift	
0·02	0·001	1·256	0·330	0·055	−0·045	0·057	a
		1·158		0·249	−0·053	0·214	b
0·02	0·0005	1·2501	0·328	0·060	−0·059	0·110	a
		1·242		0·181	−0·083	0·169	b
0·05	0·001	1·244	0·319	0·046	−0·017	0·032	a
		1·249		0·118	−0·013	0·091	b
0·05	0·0005	1·246	0·320	0·048	−0·053	0·092	a
		1·272		0·084	−0·069	0·086	b
0·1	0·001	1·253	0·319	0·047	−0·021	0·065	a
		1·265		0·070	−0·018	0·090	b

[a] Calculated by the QN method
[b] Calculated from pressure and skin friction forces

Table II. Strouhal numbers for $Re = 60$–180 with zero blockage

Re	60	100	140	180
Computed Strouhal number	0·139	0·166	0·180	0·192
Experimental Strouhal number[10]	0·135	0·164	0·180	0·191
Experimental Strouhal number[11]	0·136	0·166	0·183	—

The above values were computed with an outer radius of 200 and 200 radial segments. At $Re = 100$ the Strouhal numbers were 0·165 and 0·168 with outer radii of 120 and 400, respectively

Before considering the question of blockage, Strouhal numbers using the polar mesh alone with effectively zero blockage are shown in Table II for $Re = 60$, 100, 140 and 180, a range for which the Strouhal number is changing markedly. For these runs, $\Delta t = 0{\cdot}05$ and $\Delta\Gamma = 0{\cdot}001$ were chosen since the evidence above indicates that smaller values have an insignificant influence on the results. An outer polar mesh radius, R_{outer}, of 200 was used as discussed below. The flow asymmetry is promoted by including an onset velocity of unity in the cross-flow direction up to time 1·0, after which it is set to zero. The computations were taken to time 100 and the lift frequency used to define the Strouhal number is the average value between time 50 and 100. There have recently been several experimental investigations into flows at these Reynolds numbers[10,11] and it is accepted that vortex shedding may be produced which is almost perfectly two-dimensional up to $Re = 160$–180. Strouhal numbers (but not forces) for these conditions have been measured and are included in Table II. The agreement with our computations is seen to be very

close. Other computations where numerical convergence is claimed have been made using finite-element[12] and spectral[13,14] methods. In some cases, however, blockage could be significant and they are considered below. In Table II Strouhal numbers with $r_{outer}=120$ and 400 for $Re=100$ are also stated and are seen to be very close to that with $r_{outer}=200$, indicating that neither the proximity of the outer mesh boundary to the cylinder nor the proximity of the wake to the downstream boundary has a significant influence. The influence on forces was similarly insignificant.

Figure 2 shows Strouhal numbers for $Re=100$ with blockage using the overlapping mesh system. Increasing the blockage (reducing the blockage ratio) is seen to increase the Strouhal number down to a blockage ratio of about 4, while a blockage ratio of 2 has a lower Strouhal number than a blockage ratio of 4. These low values are included for general interest but are, apart from our general concern about the effect of large blockage ratio values (greater than 8, say). It should be emphasized that the boundary layers on the side walls are not included in the numerical simulation and they could be significant for these low blockage ratios in practice. In Figure 2 the value of 0·163 from Chaplin's[13] spectral method computation with effectively zero blockage is shown; this compares with 0·166 from the random-vortex method. The converged finite-element computation using the commerical code FIDAP[12] gives a Strouhal number of 0·173 with a blockage ratio of 16, in agreement with the random-vortex method. Results from spectral element computations[14] are also shown in Figure 2. With a blockage ratio (B) of 24, the Strouhal number is very close to the curve fitting the random-vortex values with $B \geqslant 8$ (the curve is given by $S=0{\cdot}166+0{\cdot}0516\exp(-0{\cdot}1248B)$). However, with $6 \leqslant B \leqslant 12$, values are as much as 0·004 below this curve. For the spectral element computations, however, the outer mesh is a semicircle upstream of the cylinder, and parallel side walls are thus only strictly imposed

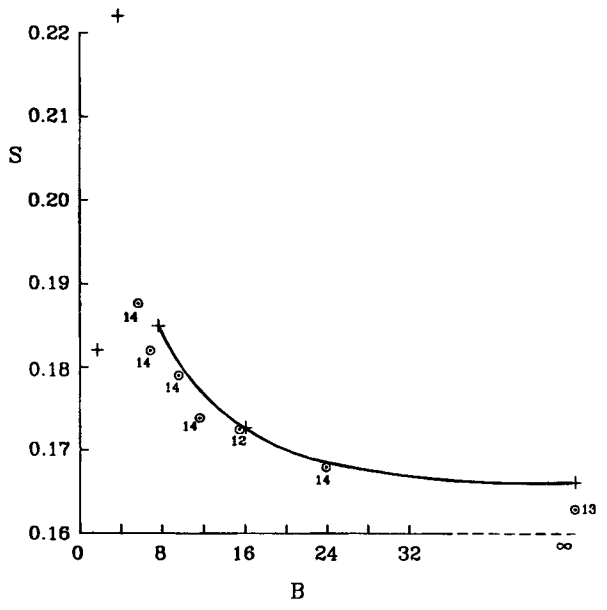

Figure 2. Variation of Strouhal number S with blockage ratio B at $Re=100$: (+) random-vortex method; (⊙[12]) finite-element method of Reference 12; (⊙[13]) spectral finite-difference method of Reference 13; (⊙[14]) spectral element method of Reference 14

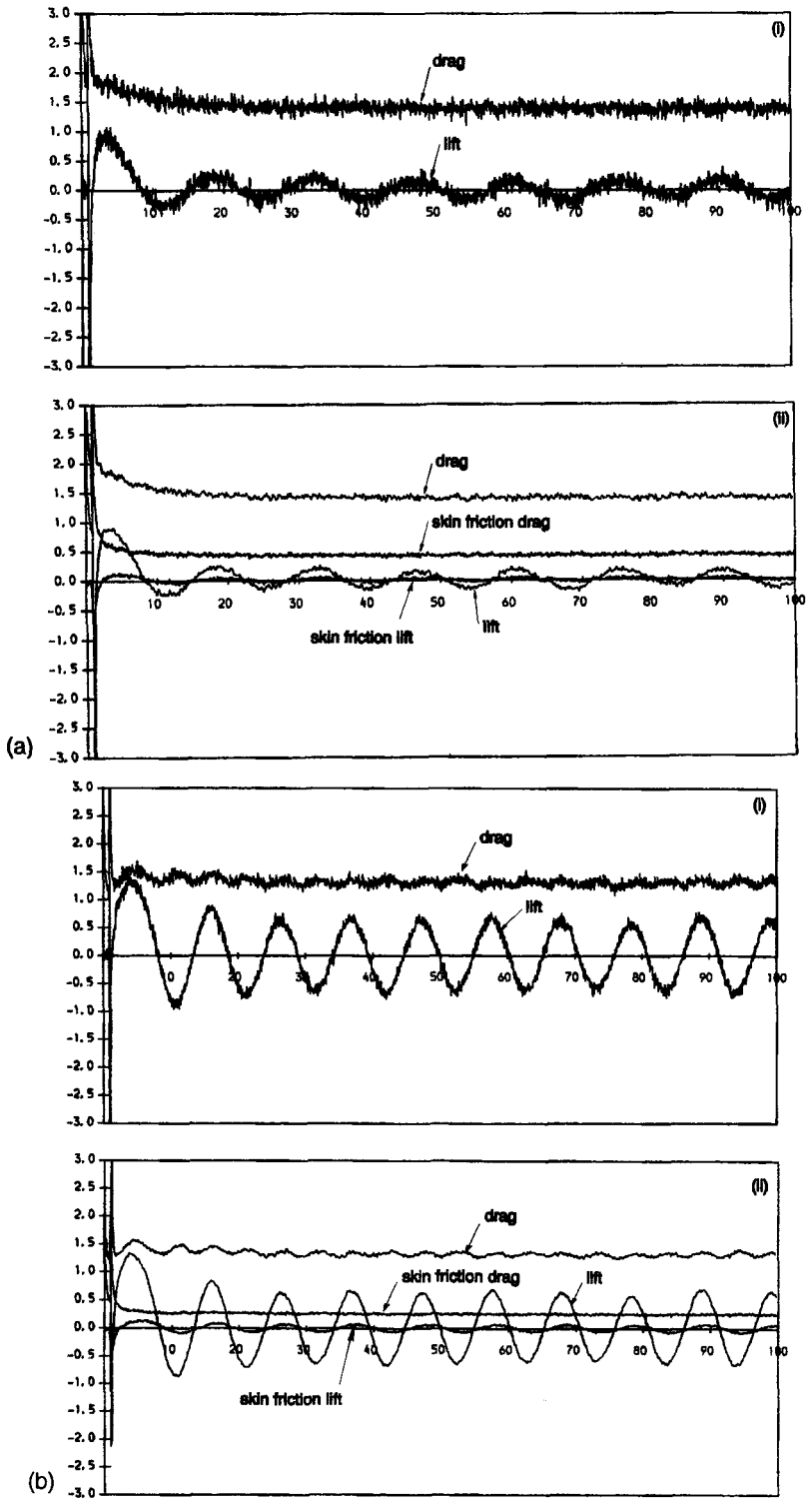

Figure 3. Force variation with time. (a) $Re = 60$: (i) drag and lift from pressure and skin friction calculation; (ii) drag and lift from the QN method and skin friction drag and lift. (b) $Re = 180$: (i) drag and lift from pressure and skin friction calculation; (ii) drag and lift from the QN method and skin friction drag and lift

downstream of the cylinder. Overall, it may be concluded that there is very close agreement for Strouhal numbers between different numerical schemes and experiment when blockage is taken into account.

We now consider the forces. Examples of force–time histories from the random-vortex method are shown in Figure 3(a) for $Re=60$ and in Figure 3(b) for $Re=180$, both with zero blockage. Forces calculated by the QN approach and through the conventional pressure and skin friction integration are shown and the random noise for the former is shown to be much less. Values of mean drag, mean skin friction drag, rms fluctuating drag, rms lift and mean lift for time 50–100 are given in Table III for different blockage ratios with $Re=100$. The rms forces from the QN method are slightly below those from the conventional force calculation, which includes greater random noise. The small differences in mean drag given by the two methods, always less than 2 per cent, remain unexplained. Results from the finite-element method with a blockage ratio of 16[12] and the spectral method[13] with zero blockage are also given. For the former the mean drag

Table III. Forces and Strouhal number with blockage at $Re=100$

Blockage ratio	Strouhal number	Mean drag	Mean skin friction drag	Rms drag	Mean lift	Rms lift	
∞	0·166	1·329	0·339	0·034	0·011	0·243	a
		1·317		0·064	0·003	0·248	b
	0·163	1·302	0·337	0·006	0·000	0·221	Reference 13
16	0·173	1·359	0·338	0·042	−0·006	0·229	a
		1·343		0·106	−0·005	0·236	b
	0·173	1·411		0·009		0·257	Reference 12
8	0·185	1·472	0·358	0·043	−0·011	0·260	a
		1·452		0·114	−0·014	0·266	b
4	0·222	1·910	0·439	0·054	−0·048	0·394	a
		1·896		0·123	−0·056	0·408	b
2	0·182	4·130	0·776	0·104	−0·034	0·772	a
		4·216		0·175	−0·003	0·828	b

[a] Calculated by the QN method
[b] Calculated from pressure and skin friction forces

Table IV. Forces and Strouhal number for $Re=60$–180 with zero blockage

Ref	Strouhal number	Mean drag	Mean skin friction drag	Rms drag	Mean lift	Rms lift	
60	0·139	1·404	0·429	0·028	0·008	0·112	a
		1·389		0·076	−0·003	0·139	b
100	0·166	1·329	0·339	0·034	0·011	0·243	a
		1·317		0·064	0·003	0·248	b
140	0·180	1.313	0·292	0·027	0·008	0·351	a
		1·303		0·060	0·001	0·355	b
180	0·192	1·327	0·263	0·034	0·004	0·451	a
		1·316		0·065	−0·003	0·454	b

[a] Calculated by the QN method
[b] Calculated from pressure and skin friction forces

and rms lift are 4 and 12 per cent, respectively, greater than for the random-vortex method. In contrast, the values for the spectral method were lower by 2 and 10 per cent, respectively. In general, the agreement for the forces is less close than for the Strouhal numbers and there are no comparable experimental measurements.

To complete the picture, forces with $Re=60$, 100, 140 and 180 and zero blockage are given in Table IV. While we are unaware of relevant values from other computations, these values should be useful for future comparison. We also show streamline plots for $Re=60$ and 180 in Figure 4. The rolling-up of the separated shear layers in the near wake is very much closer to the cylinder for $Re=180$ than for $Re=60$ which experiences a correspondingly smaller fluctuating lift force.

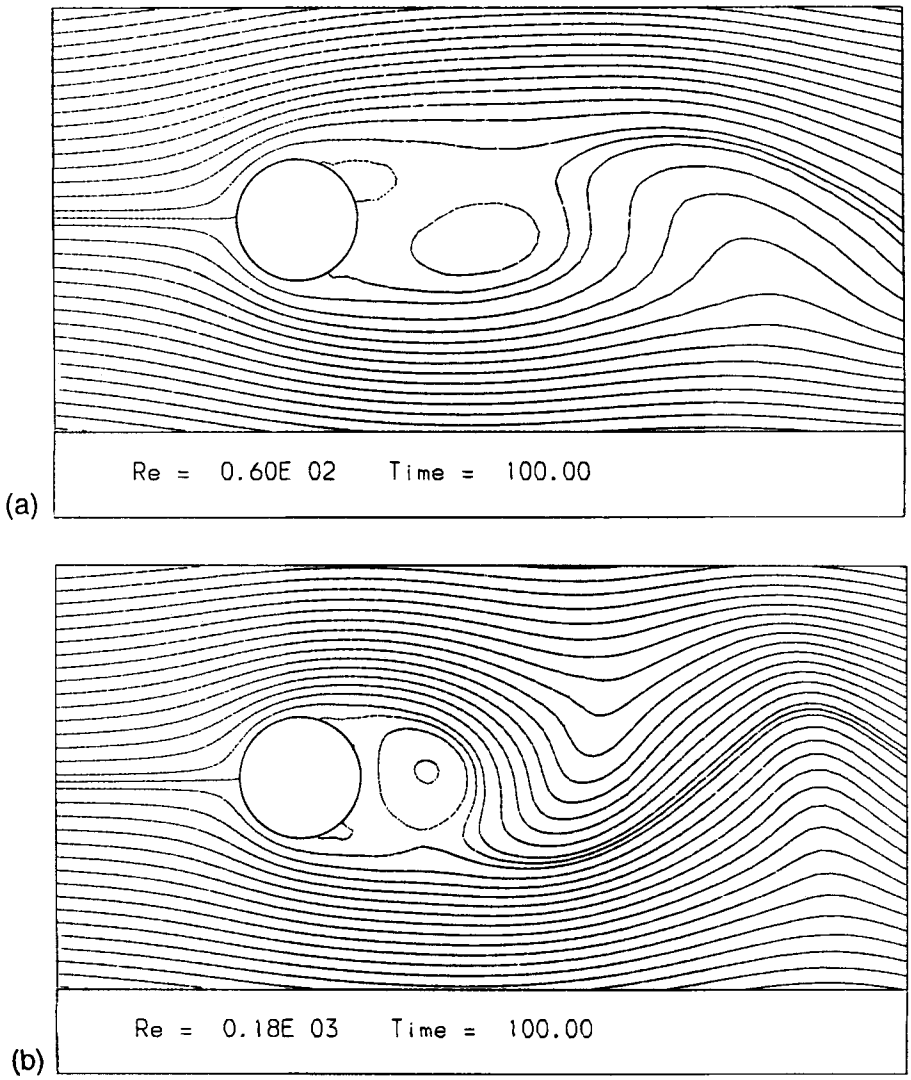

Figure 4. Typical streamline plots for stream function values at intervals of 0·2 including the central upstream streamline: (a) $Re=60$; (b) $Re=180$

In attempting to understand differences in the results between different numerical schemes, it would be useful to compare streamline plots associated with specific phases of lift force fluctuation. However, this was not available for this study.

CONCLUSIONS

Different numerical schemes are seen to give very close agreement in Strouhal numbers at $Re = 100$ when blockage is taken into account. Also, values for $60 \leqslant Re \leqslant 180$ are seen to be in very close agreement with experiments where the flow is shown to be effectively two-dimensional.

Different numerical schemes, however, give less close agreement in forces and there are no comparable experimental results. The fluctuating lift, in particular, can show significant differences from one scheme to another, up to 22 per cent, and clearly this should be an area for further investigation.

The computations with the random-vortex method show how increasing blockage affects the Strouhal number and forces. The effect is substantial for small blockage ratios, say less than 8. With large blockage ratios the conventional blockage correction for steady flow might be thought to apply. With a ratio of 16 this would predict an effective increase in onset velocity of about 4 per cent above that for zero blockage and the Strouhal number does in fact change accordingly. However, the forces show little change. Mean drag is increased by about 2 per cent while rms lift is slightly decreased. This is in apparent contrast to experiments at higher Reynolds numbers (10^3–10^5), where a plot of base pressure coefficient against Reynolds number has been shown to be close to a single curve when blockage ratios between 14 and 56 were corrected for.[17]

ACKNOWLEDGEMENTS

This paper is part of a project supported through the Marine Technology Directorate's managed programme on the Behaviour of Fixed and Compliant Offshore Structures which is sponsored by SERC, Amoco, BP, Elf, Statoil, Admiralty Research Establishment, Brown and Root Marine and Aker Engineering.

APPENDIX: NOTATION

B	blockage ratio, distance between the upper and lower boundaries divided by cylinder diameter
F_x	force in the x direction (drag)
F_{xs}	skin friction force in the x direction
F_y	force in the y direction (lift)
F_{ys}	skin friction force in the y direction
r	radial co-ordinate
Re	Reynolds number based on cylinder diameter
S	Strouhal number also based on cylinder diameter
t	time
$\mathbf{u}$	velocity vector
u, v	velocity components in the x and y directions
x, y	Cartesian co-ordinates, x is distance downstream of cylinder centre
Γ	circulation
Δt	time step
$\Delta\Gamma$	maximum circulation magnitude of point vortex

ψ stream function
θ angular co-ordinate
ω vorticity

REFERENCES

1. W. M. Collins and S. C. R. Dennis, 'Flow past an impulsively started cylinder', *J. Fluid Mech.*, **60**, 105 (1973).
2. P. Justesen, 'A numerical study of oscillating flow around a circular cylinder', *J. Fluid Mech.*, **222**, 157 (1991).
3. Ta Phuoc Loc and R. Bouard, 'Numerical simulation of the early stage of the unsteady viscous flow around a circular cylinder: a comparison of experimental visualisation and measurements', *J. Fluid Mech.*, **160**, 93 (1985).
4. A. Y. Cheer, 'Unsteady separated wake behind an impulsively started cylinder in slightly viscous flow', *J. Fluid Mech.*, **201**, 485 (1989).
5. P. A. Smith and P. K. Stansby, 'Impulsively started flow around a circular cylinder by the vortex method', *J. Fluid Mech.*, **194**, 45 (1988).
6. P. A. Smith and P. K. Stansby, 'An efficient surface algorithm for random-particle simulation of vorticity and heat transport', *J. Comput. Phys.*, **81**, 349 (1989).
7. W. M. Collins and S. C. R. Dennis, 'The initial flow past an impulsively started circular cylinder', *Q. J. Mech. Appl. Math.*, **26**, 53 (1973).
8. M. Bar-Lev and H. T. Yang, 'Initial flow field over an impulsively started cylinder', *J. Fluid Mech.*, **72**, 625 (1975).
9. R. Bouard and M. Coutanceau, 'The early stage of development of the wake behind an impulsively started cylinder for $40 < Re < 10^{4}$', *J. Fluid Mech.*, **101**, 583 (1980).
10. C. H. K. Williamson, 'Oblique and parallel modes of vortex shedding in the wake of a circular cylinder at low Reynolds numbers', *J. Fluid Mech.*, **206**, 579 (1989).
11. M. Hammache and M. Gharib, 'An experimental study of the parallel and oblique vortex shedding from circular cylinders', *J. Fluid Mech.*, **232**, 567 (1991).
12. M. S. Engelman and M.-A. Jamnia, 'Transient flow past a circular cylinder: a benchmark slution', *Int. j. numer methods fluids*, **11**, 985 (1990).
13. J. R. Chaplin, private communication, 1992; the numerical method is described in J. R. Chaplin 'Orbital flow around a circular cylinder. Part 2. Attached flow at large amplitudes', *J. Fluid Mech.*, **246**, 397 (1993).
14. G. Em Karniadakis and G. S. Triantafyllou, 'Three-dimensional dynamics and transition to turbulence in the wake of bluff objects', *J. Fluid Mech.*, **238**, 1 (1992).
15. A. Slaouti and P. K. Stansby, 'Flow around two circular cylinders by the vortex method', *J. Fluids Struct.*, **6**, 641 (1992).
16. E. C. Maskell, 'A theory of the blockage effects on bluff bodies and stalled wings in a closed return wind tunnel', *Aero. Res. Coun.*, R and M 3400.
17. P. K. Stansby, 'Vortex wakes of circular cylinders oscillating in uniform and sheared flows', *Ph.D. Dissertation*, University of Cambridge, 1974.
18. A. J. Chorin, 'Numerical study of slightly viscous flow', *J. Fluid Mech.*, **57**, 785 (1973).
19. O. Hald, 'The convergence of vortex methods', *SIAM J. Numer. Anal.*, **16**, 726 (1979).
20. H. Lamb, *Hydrodynamics*, 7th edn., Cambridge University Press, Cambridge, 1975.
21. L. Quartepelle and M. Napolitano, 'Force and moment in incompressible flows', *AIAA J.*, **21**, 911 (1983).
22. P. A. Smith and P. K. Stansby, 'Viscous oscillatory flows around cylindrical bodies at low Keulegan–Carpenter numbers using the vortex method', *J. Fluids Struct.*, **5**, 339 (1991).